Chapter 1

The Pilot Contamination problem

Author Name (Cristina Gava)
Student ID 1153449

1.1 Overview

Compared to existing cellular network infrastructures, nowadays there is an increasing need for technologies providing higher capacity. This comes from an always bigger demand for higher data rates in wireless mobile communication systems such as Internet if Things (IoT), Machine to Machine (M2M) communication and other electronic services.

The current Fourth Generation (4G) cellular networks, 3rd Generation Partnership Program (3GPP) above all, were designed with the intention to support a peak spectral efficiency of 15 bps/Hz, a bandwidth of 100 MHz and an ultra-low latency. Nonetheless, the estimated future traffic far exceeds the resources of the current 4G and so the need for 5G cellular networks.

One of the novelties of the 5G protocol, which is beeing designed and refined in the present communication scenario, is the Multiple-input Multiple-output (MIMO) system, a technology that focuses on the idea of implementing multiple antennas terminals in one device - or Base Station (BS) - in order to enhance the communication quality and reliabilty. Without going into details, one of the options for this system is the multiuser MIMO system, where an array of antennas serves a group of autonomous terminals at the same time. These terminals may be single-antenna cheap devices and the

multiplexing throughput gains are shared among the User Terminal (UT)s [1] [2].

In this type of system, the Channel State Information (CSI) has a crucial role, since forward-link data transmission needs that the base station know the forward channel, as well as the reverse-link data transmission require it to know the reverse channel. This is the reason why such things as pilot signals exist, but with them some problems might arise due to the contamination of such signals. What we mean to takle in this chapter are exactly those kind of problems, referred to as pilot contamination, and at a couple of main approaches to solve them.

1.2 The pilot contamination problem

In several works multi-user MIMO operations with a big excess of base station antennas are considered: in them the channel is estimated exploiting the feedback or channel reciprocity schemes through multiplexing over frequency - Frequency Division Duplex (FDD) - or over time - Time Division Duplex (TDD). In TDD a time-slot, over which the channel can be thought as constant, is divided between reverse-link pilots and forward-link data transmission. The pilots assume reciprocity of the channel to provide the BS with an estimate of the forward channel, which in turn generates a linear pre-coder for data transmission [1]. In the FDD scenario the division is made over the frequency and the system requires not only the estimation, but also feedbacks for both forward and reverse direction between the BS and the UT.

For this reason TDD is considered a more suitable approach than the FDD when it comes to acquiring CSI in wireless systems [2]. Following this line, we will focus on this system.

In TDD the time pilots require is proportional to the number of terminals served, whereas the number of base station antennas does not influence it. At the same time, though, the number of terminals that can be served is limited by the coherence time. One of the principal findings in this sense is that the addition of BS antennas always brings benefits to the SNR situation.

To simplify the observed scenario, several works focus on multi-user MIMO operations with an infinite number of base station antennas in a multicellular environment. In general, in a MIMO system, when the UTs transmit their pilot sequences to the BS in order to perform the channel estimation in the Uplink (UL) training phase, every BS not only learns

the channel related to the intended UT, but also fractions of the channels connected to other UTs that happen to have pilots related to the ones used by the intended UT.

1.2.1 UL training

The use of pilot in the TDD scheme is related to the Uplink segment training. Considering the worst-case scenario in this means assuming that all the T single-antenna UTs transmit synchronous pilot sequences of length τ symbols at the beginning of every coherence interval. Every j^{th} cell then transmits a $\tau \times T$ orthogonal matrix $\mathbf{S}_j = (\mathbf{s}_{j1}, \ldots, \mathbf{s}_{jk})$ which satisfies $\mathbf{S}_j^T \mathbf{S}_j = \tau \mathbf{I}$. The received signal matrix at the l_{th} BS is then:

$$\mathbf{Y}_l = \sqrt{p_u} \sum_{j=1}^{L} \mathbf{D}_{l,j}^{1/2} \mathbf{H}_{l,j} \mathbf{S}_j^T + \mathbf{N}_l \tag{1.21}$$

with:

- $\mathbf{N}_l$ = the $R \times \tau$ additive noise matrix whose elements are are i.i.d. zero mean, circularly-symmetric complex gaussian $\mathcal{CN}(0,1)$ random variables and R is the number of antennas at the ase station;

- p_u = the average transmit power for each user on the uplink and is a measure of pilot signal-to-noise ratio;

At the same time, the two matrices:

$$\mathbf{D}_{l,j} = \begin{pmatrix} \beta_{l,1,j} & & \\ & \ddots & \\ & & \beta_{l,T,j} \end{pmatrix} \quad \textbf{and} \quad \mathbf{H}_{l,j} = \begin{pmatrix} h_{l,1,j,1} & \ldots & h_{l,T,j,1} \\ \vdots & \ddots & \vdots \\ h_{l,1,j,R} & \ldots & h_{l,T,j,R} \end{pmatrix}$$

are the matrices respectively of the large scale fading coefficients and of the small scale fading factors, whose variables are $\mathcal{CN}(0,1)$.

1.3 The main sources of contamination

Pilot conatmination can be related to two main causes: non-orthogonal pilot schemes and hardware impairments. While the first source is the most common and known one, the second source has been considered only recently and is still gaining consideration.

1.3.1 Non orthogonal pilot schemes

Normally, in a multi-cell system where the same frequency is shared by L users, pilots are assumed to be mutually orthogonal and hence the intra-cell intereference is considered negligible. However, when frequency reuse comes into play, these signals are affected by this intereference, resulting in pilot contamination. In this case, the expression for the received signal is the same as in 1.21 [2].

The conclusion of inter-cell interference was reached already by Marzetta in [1], where he precisely excluded the other possible sources of intra-cell interference and shadow fading. The author starts from the already considered propagation model where the single-antenna terminals are randomly distributed over the cell and separated by hundreds of wavelengths. Under these assumptions, the propagation vectors between the base station and the different terminals would be uncorrelated, since for a sufficiently high number of elements in a base station array the typical angular spacing between any two terminals would be greater than the angular Rayleigh resolution of the array, resulting in asymptotically orthogonal propagation vectors for different terminals. In fact, it can be shown that the inner product between two propagation vectors of any two terminals has a standard deviation of $\sqrt{R}$ (with R being the number of antennas at the BS) and it is the same we would get with independent Rayleigh fading. Instead from the channel linear estimation, the L2-norm of a propagation vector is equal to R and so, as the number of base station antennas grows, this inner products between two different propagation vectors grows at a lower pace than the inner products of propagation vectors with themselves.

Therefore, the intra-cell intereference, the fast fading and the additive receiver noise effect disappear, leaving the inter-cell interference as the only remaning obstacle.

In this context the author analiyzes the transmission scenario where he considers:

- Hexagonal cells;
- Orthogonal Frequency Division Multiplexing (OFDM) modulation;
- Unlimited number of antennas per BS;
- Single antennas terminals;
- TDD.

In this work there is a maximum number of terminals for which the BS can learn the channel: it is limited by the time it takes to acquire the CSI from the moving terminals, specifically $T_{max} = \tau N_{smooth}$ with τ the number of OFDM symbols and N_{smooth} the number of subcarriers over which the channel response is constant. The implication is that, in general, pilots from different cells are non-orthogonal, unless $T \cdot L \leq \tau N_{smooth}$ is true for T pilots per cell. The author first analyzes the problem with the constraint of having the same set of T pilots used among the L cells, in this way guaranteing intra-cell orthogonality, ut not inter-cell one; he later focuses on the case of a set of pilots independents in both the cases. The main conclusion of his apporach is that, through linear channel estimation, pilot contamination is something inherent to the system asrchitecture in such a way that a non-aggressive frequency reuse is a more effective measure, since in the second case, despite a non significant difference in Signal-to-Interference Ratio (SIR) with respect to the first case, the mean throughput per cell will suffer [1].

1.3.2 Hardware impairments

Some works studied the impairments that some hardware components in radio frequency chain are prone to; these impairments can affect the accuracy of the Channel Estimation (CE) with related pilot contamination. These works approached this contamination source through modeling some sort of non-ideal behavior of each component, but with more attention to the system overall response. In general, one main study [3] shows how the hardware impairments from the BS are negligible, while the main component of it comes from the UTs, which limit the capacity in massive MIMO systems as M grows large. In this scenario, and considering the deterministic pilot signal $d \in \mathbb{C}$, the UL non-ideal system model that takes into consideration the distorsion noise for the received signal $\mathbf{y} \in \mathbb{C}$ at the BS is represented by:

$$\mathbf{y} = \mathbf{g}(d + \eta_t^{UT}) + \boldsymbol{\eta}_r^{BS} + \mathbf{v} \tag{1.32}$$

Where the stochastic processes $\eta_t^{UT} \in \mathbb{C}$ and $\boldsymbol{\eta}_r^{BS} \in \mathbb{C}^{M\times 1}$ describe the impairments of the transmitter and the receiver hardware at the UT and the BS respectively. Whereas the ergodic process which is the additive noise $\mathbf{v} = \mathbf{v}_{noise} + \mathbf{v}_{interf} \in \mathbb{C}^{M\times 1}$ consists of independent receiver noise $\mathbf{v}_{noise} \sim \mathcal{CN}(\mathbf{0}, \sigma_{BS}^2\mathbf{I})$ and potential interference from other simultaneous transmissions.

1.3.3 Effects of pilot contamination

The considered effects can be analyzed first by the formulation of SIR expressions that can subsequently be translated into achievable rates; As much as Signal-to-Interference plus Noise Ratio (SINR) can be considered, which has been demonstrated to saturate as M tends to infinity both in the uplink and in the downlink segment [2] [4]. At the same time system performance degrades visibly because of pilot contamination when the inter-cell interference factor β, composed by shadow fading and path loss, increases [2].

1.4 Schemes for pilot contamination mitigation

There are several existing methods which intend to eliminate or mitigate the effects of pilot contamination, in particular for the case of TDD systems. The two main categories these solutions have been divided in are, namely, the pilot-based estimation approach and the subspace estimation approach. Below we will give a brief explanation of what the former method consists of, whereas we will present one solution for the latter.

1.4.1 The pilot-based approach

In this approach, the main idea is that non-orthogonal pilots are used across the cells, while orthogonal ones within the cell. Through this assumption it was possible, for example, to transmit pilot signals from different cells by shifting the pilot location in frames so that users in separate cells transmit without overlapping in time. Another point of view is using precoding methods requiring a limited collaboration among the BSs [2].

1.4.2 The subspace-based approach

The strength of this approach is that it requires very few pilot symbols per operation. In these, CSI is obtained through the application of Eigenvalue Decomposition (EVD) on the covariance matrix of the received samples. Moreover, since it is not true a priori that the desired channels are always stronger than the interfering channels, Maximum a-posteriori (MAP) criteria were added to it in some approaches.

The solution we briefly consider here was elaborated by Müller *et al.* in [5] and consists of a *nonlinear* channel estimation based on a subspace projection.

One of the most important statements of the paper is the confutation of the conclusion drawn by Marzetta *et al.* in [1], where they stated that the array gain cannot be achieved for channel estimation, but only for data detection. Disproving this, [5] uses this gain for the nonlinear channel estimation algorithm, as well as shows how pilot contamination is a consequence of *linear* channel estimation and not a fundamental effect that cannot be removed.

System model

The work considers a wireless communication channel in the UL, with the channel bandwith smaller than the coherence bandwidth, and the channel being frequency-flat, block-fading and narrowband. Let the number of trasmit antennas be T and the number of receiving antennas $R > T$. In this context, we can elaborate the Code Division Multiple Access (CDMA) system:

$$\mathbf{Y} = \mathbf{H}\mathbf{X} + \mathbf{Z}, \tag{1.43}$$

where:

- $\mathbf{X} \in \mathbb{C}^{T \times C}$ is the transmitted data;
- $\mathbf{Y} \in \mathbb{C}^{R \times C}$ is the received signal;
- $\mathbf{Z} \in \mathbb{C}^{R \times C}$ is the additive noise;
- $\mathbf{H} \in \mathbb{C}^{R \times T}$ is the channel matrix, whose columns denote the spreading sequences;

Therefore we can deploy the well-know fact that there is no need to know the spreading sequences - needed to demodulate the CDMA - to come up with the so-called blind approach described below.

The proposed method

The proposed algorithm states that it might be a good idea not to estimate the channel matrix $\mathbf{H}$, but directly consider the subspace channel:

$$\tilde{\mathbf{Y}} = \tilde{\mathbf{H}}\mathbf{X} + \tilde{\mathbf{Z}} \tag{1.44}$$

and estimate the much smaller subspace channel matrix $\tilde{\mathbf{H}} \in \mathbb{C}^{T \times T}$.

This because only the largest eigenvalues of $\mathbf{Y}\mathbf{Y}^T$ are necessary to our purpose. Precisely, considering the case of $T = 1$ active transmit antenna

and looking for the matched filter m^T such that the Signal to Noise Ratio (SNR) at its output is maximum, we are looking for maximizing the total received power normalized to the power gain of the filter. Formally:

$$\mathbf{m} = \underset{\mathbf{m}}{\operatorname{argmax}} \frac{\mathbf{m}^\dagger \mathbf{Y}\mathbf{Y}^\dagger \mathbf{m}}{\mathbf{m}^\dagger \mathbf{m}} \tag{1.45}$$

In such case, the maximum value is exactly given by the maximum eigenvalue of $\mathbf{Y}\mathbf{Y}^\dagger$, for an algebraic result.

If we now extend this idea to the case of multiple transmit antennas, we can see that the subspace of eigenvalues we need is given by the projection of the received signal onto the signal space basis $\mathbf{S}^T \in \mathbb{C}^{T\times R}$. This quantity derives from the matrix of left singular vectors obtained by Singular Value Decomposition (SVD) on $\mathbf{Y}$. To express it in a more formal way we have:

$$\mathbf{Y} = \mathbf{U}\mathbf{\Sigma}\mathbf{V}^\dagger \tag{1.46}$$

with unitary matrices $\mathbf{U} \in \mathbb{C}^{R\times R}$ and $\mathbf{V} \in \mathbb{C}^{C\times C}$, and the diagonal matrix $\mathbf{\Sigma} \in \mathbb{C}^{R\times C}$ with diagonal entries sorted in non-increasing order. Based on this the $\mathbf{U}$ matrix has the structure:

$$\mathbf{U} = [\mathbf{S}|\mathbf{N}] \tag{1.47}$$

with the null space basis being $\mathbf{N} \in \mathbb{C}^{R\times(R-T)}$.

The projection in question is thus expressed as:

$$\tilde{\mathbf{Y}} = \mathbf{S}^\dagger \mathbf{Y} \tag{1.48}$$

About the white noise we can remark that if then we consider the case of massive MIMO scenario, where $R \gg T$, then we see that the influence of it onto the signal subspace becomes negligible as $R \to \infty$. This because white noise is evenly distributed in all the dimensions of the full space, which in turn is much bigger than the T-dimensional signal subspace.

What is left to see then is the co-channel interference from L neighboring cells, which typically is not white and jusitfies the relation for which the more colored the smaller the *load* factor:

$$\alpha = \frac{T}{R} \tag{1.49}$$

Were we able to identify which singular values correspond to channel vectors from inside the cell, as opposed to the ones from neighboring cells, we could

try to remove them by subspace projection. Moreover we keep also in mind that any R-dimensional channel vector from any transmitter to the receiver in the interested cell is orthogonal to any other channel vector. Therefore we can conclude that in a cellular system with power-controlled handoff strategy, the norm of channel vectors from neighboring cells can never be bigger than the norm of interested-cell channel vectors; this means that we can identify the singular values belonging to transmitters internal to the cell by ordering them by magnitude [5].

Performance ananlysis

In the frame of classical massive MIMO settings, with L finite, $R, T \to \infty$ and $0 \neq \alpha \ll 1$, the impairment process $\mathbf{Z}$ is composed by a white noise component $\mathbf{W}$ (having iid elements with zero mean and variance W) and the interference from L neighboring cells:

$$\mathbf{Z} = \mathbf{W} + \mathbf{H}_I \mathbf{X}_I \tag{1.410}$$

Also the definition of the normalized coherence time comes in our help:

$$\kappa = \frac{C}{R} \tag{1.411}$$

In the large antenna limit $R \to \infty$, if we consider that the singular values of the normalized noise $\frac{\mathbf{W}}{\sqrt{CW}}$ are bounded by the interval

$$\frac{1}{\sqrt{\kappa}} - 1 < x < \frac{1}{\sqrt{\kappa}} + 1 \tag{1.412}$$

we can say that, at most, the power of white noise being present in $\tilde{\mathbf{Y}}$ is:

$$Noise_w = \left(\left(\frac{\mathbf{W}}{\sqrt{CW}} \right) \sqrt{CW} \right)^2 = CW \left(1 + \frac{1}{\sqrt{\kappa}} \right)^2 \tag{1.413}$$

for one singular value, while it is

$$TNoise_w \tag{1.414}$$

in the worst case, where the T largest singular values of the noise affect the signal of interest.

To then calculate the SNR in $\tilde{\mathbf{Y}}$ we can give an espression for the total power of the received signal as $TRCP$, since the data signal $\mathbf{X}$ is iid zero

mean with variance P (which account for its power). The SNR can be thus lower bounded by:

$$SNR \geq \frac{P}{W} \frac{R}{\left(1+\frac{1}{\sqrt{\kappa}}\right)^2} \tag{1.415}$$

As mentioned at the beginning of this section, there is also the co-channel interference from neighboring cells. This quantity is not white but at the same time higly concentrated in certain subspaces and can be suppressed making use of the phase transition of spectra of large random matrices. Indeed in [6] the authors show how, in a multi-user MIMO scenario, the eigenvalue distribution of $\mathbf{H}$, when properly scaled or shifted, parts into two separate non-overlapping bulks with each bulk being shaped very similar to the cases of pure scattering and pure line-of-sight. This comes to help when trying to separate the co-channel interference (the equivalent of the pure scattering) from the normalized signal of interest $\frac{\mathbf{HX}}{\sqrt{TR}}$ (the equivalent of pure line-of-sight).

For this we start observing that in the appendix A of [5], the signal of interest is shown to converge to:

$$\mathcal{P} = \left[\frac{\kappa P}{\alpha} - 2P\sqrt{\frac{\kappa^2+\kappa}{\alpha}}; \frac{\kappa P}{\alpha} + 2P\sqrt{\frac{\kappa^2+\kappa}{\alpha}}\right] \tag{1.416}$$

as $R \to \infty$ and for $\alpha \ll 1$.

We then proceed supposing the entries of the matrix of interfering signals $\mathbf{X}_I$ be iid with zero mean and variance P, while the entries of the matrix of interfering channels $\mathbf{H}_I$ be iid with zero mean and variance I/P. In this way the ratio accounts for the relative attenuation between the intercell users and users external to the cell. Thus the empirical distribution of the squared singular values of the normalized co-channel interference ($\frac{\mathbf{H}_I\mathbf{X}_I}{\sqrt{TR}}$) converges to a limit distribution as well. This distribution, for $\alpha \ll 1$ is supported in the interval

$$\mathcal{I} = \left[\frac{\kappa I}{\alpha} - 2I\sqrt{L\frac{\kappa^2+\kappa}{\alpha}}; \frac{\kappa I}{\alpha} + 2I\sqrt{L\frac{\kappa^2+\kappa}{\alpha}}\right] \tag{1.417}$$

Therefore, having obtained two intervals (and so relative upper bounds) on the signal received and the co-channel interference, we can make use of the statement in [6] to affirm that if these two intervals do not overlap, i.e.

$$\mathcal{P} \cap \mathcal{I} = 0 \tag{1.418}$$

or better

$$\frac{P}{I} > \frac{1+2\sqrt{\alpha L\left(1+\frac{1}{\sqrt{\kappa}}\right)}}{1-2\sqrt{\alpha\left(1+\frac{1}{\kappa}\right)}} \overset{\alpha \ll 1}{\approx} 1+2\left(1+\sqrt{L}\right)\sqrt{\alpha\left(1+\frac{1}{\kappa}\right)} \tag{1.419}$$

then, in the limit $\alpha \to 0$ the signal bulk can always be separated from the interference bulk as long as $\frac{P}{I} > 1$. Through this it can be stated that the two subspaces, the signal and the interference one, can be identified blindly and the interference can be nulled out [5].

Results

The results of Müller *et al.* in [5] are obtained through the application of Monte-Carlo simulation for the undecoded Bit Error Rate (BER) under the hypothesis of Quaternary Phase Shift Keying (QPSK) and flat Rayleigh fading. These results have then been compared with the ones obtained by Marzetta in [1]. In Figure 1.1 the case of high SNR is considered and shows how the BER drops drastically if the reciprocal of the rate given in 1.419 is below the threshold provided by the random matrix method, confirming the possibility to overcome the pilot contamination problem.

Figure 1.4.2 represents the more relevant case, where the algorithm explained above achieves significant performance gains compared to the linear channel estimation. In the picture it is also underlined the maximum I/P ratio over which the the singular values do not separate in the simulations.

1.5 Pilot contamination and mmWaves

In this paragraph we briefly highlight a quite recent work from Naqvi *et al.* that focuses on the problem of pilot contamination in the mmWaves scenario [7].

1.5.1 The scenario

The authors use an hexagonal geometry with random deployment of users, studying a conventional frequency reuse and deriving the network throughput. The geometry and reuse model are well represented in Figure 1.3, where each

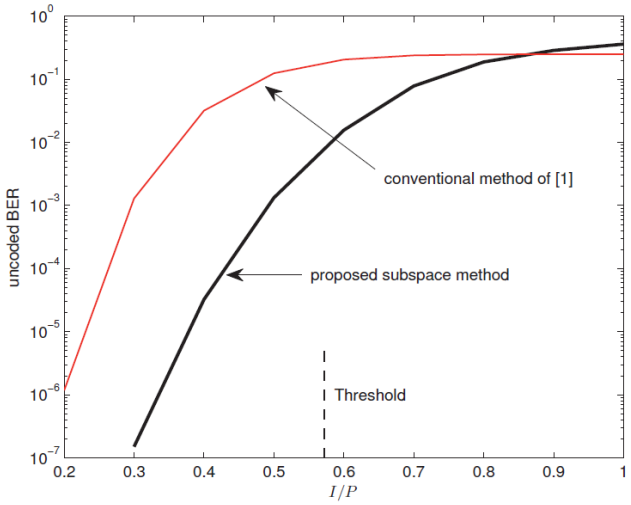

Figure 1.1: BER for 1 pilot symbol per transmit antenna and cell, $R = 400$ receive antennas, $T = 4$ transmit antennas, $L = 2$ neighboring cells, coherence time of $C = 1000$ symbols, and signal-to-noise ratio $P/W = 100$.

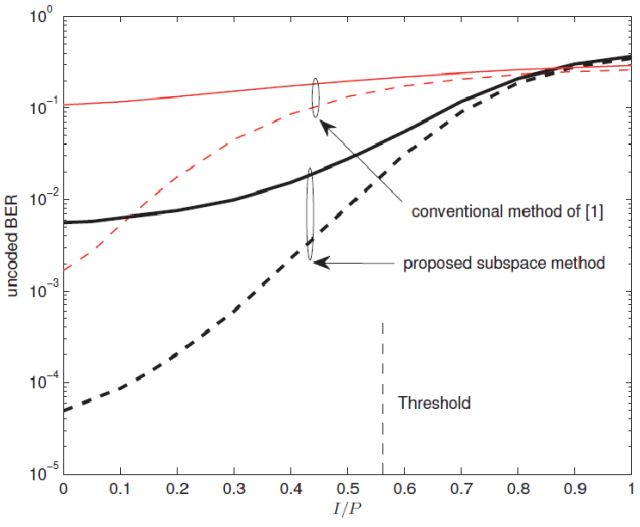

Figure 1.2: BER for $R = 200$ receive antennas, $T = 2$ transmit antennas, $L = 2$ neighboring cells, coherence time of $C = 400$ symbols, and signal-to-noise ratio $P/W = 0.1$. The solid and dashed lines refer to 1 and 10 pilot symbols per transmit antenna and cell, respectively.

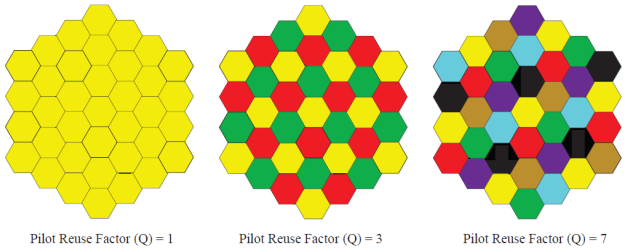

Figure 1.3: Pilot reuse under consideration

color represents a set of orthogonal pilots. These pilots are then mutually orthogonal from color to color. As usual t he total number of cell in our case is L, the reuse factor of each cell is given by the parameter $Q = \{1, 3, 4, 7, \dots\}$ and each cell contains an R-antenna BS that serves T randomly deployed single antenna mobiles.

1.5.2 Multicell UL communication

All the users in this scenario communicate with their respective BS in two stages: the UL training with pilot reuse and the actual transmission of data.

In the first stage orthogonal pilots are assigned to the users in each cell, and deploy the reuse factor Q. Specifically, assume a pre-designed pilot sequence matrix in the form:

$$\mathbf{\Psi} = [\psi_0, \psi_1, \dots, \psi_{Q-1}] \quad \in \mathbb{C}^{QT \times QT} \tag{1.520}$$

with $\mathbf{\Psi}$ being divided among the cells and its i^{th} element is assigned to the i^{th} serving cell, so that the pilot sequence is further reused by cell lQ, with $1 \leq |l| \leq \lfloor \frac{l}{Q} \rfloor$.

If we now take the case of cell 0 in a single-time frequency block, then the signals received at BS 0 are in the form:

$$\mathbf{P}_0 = \sqrt{\phi_\tau QT} \sum_{j=0}^{L-1} \mathbf{H}_{0,j} \mathbf{\Psi}^*_{(j)} + \mathbf{W}_0 \quad \in \mathbb{C}^{R \times T} \tag{1.521}$$

with, again, $\mathbf{H_{0,j}}$ being the channel matrix between the mobiles of cell j and BS 0, $\mathbf{W}_0$ being the iid $\mathcal{CN}(0, 1)$ and ϕ_τ being the average transmission power per mobile. We specify also that the factor $\sqrt{QT}$ guarantees that the average power is precisely ϕ_τ.

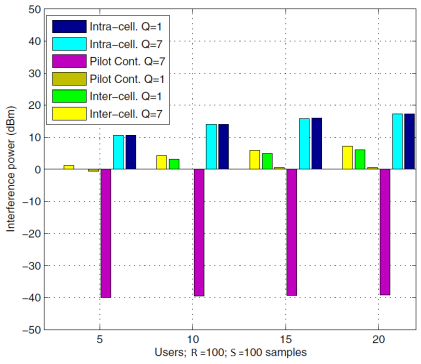

Figure 1.4: Interference components in UHF systems using $Q = 1$ and 7

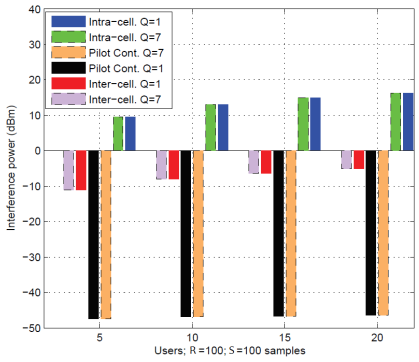

Figure 1.5: Interference components in mmWave systems using $Q = 1$ and 7

Next, the received signal is projected onto $\Psi_{0,k}$ in order to estimate the elements of $\mathbf{H_{0,j}}$ at the BS 0.

The subsequent actual transmission of data works in a similar way and the expressions obtained in [7] well distinguishes the intra-cell and the inter-cell interfernce.

Finally, the reader can look at section C in [7] for the mathematical derivation of the achievable cell throughput.

1.5.3 Results

We list here some of the most important results that come up from the work in [7]. In the first chart in Figure 1.4 we can see the interference power for the UHF link for 5, 10, 15 and 20 users per cell, and $R = 100$ antennas. We put the focus on some main aspects:

- the inter-cellular and the intra-cellular interferences increase steadily with an increase in the number of users for either value of Q. In this, since the user location is random, both the interferences have the same impact on the throughput: for closer points to the BS the intra-cell interference dominates, whereas it is the contrary for long distances;
- the pilot contamination, for the two reuse factors, has separate fixed

values that are independent of the total number of user and derive fromemthe hexagonal geometry. Thus here the number of interferers causing pilot contamination will always be 6 for any reuse factor;

- what is most interesting, though, is the aknowledgment of the pilot reuse potency, as pilot contamination falls from approximately 0 dBm for $Q = 1$, to -40 dBm for $Q = 7$. This because a greater value of the pilot reuse factor means a greater distance of the interferer from the BS. Otherwise stated, it implies a greater path loss experienced by the interfering signal, which means less pilot contamination.

In the second chart interference power for mmWave frequencies is examined. Here we see that:

- there is a correspondence in inter-cellular and intra-cellular interferences with the behavior seen in UHF systems;
- in this case, however, the inter-cell interference for both pilot reuse factors is much smaller than the one in the previous graph. The mmWave link's increased path loss gives then the advantage of dampening the interference from the neighboring cells such that a higher pilot reuse factor has no further impact on pilot contamination [7].

Summarizing what have seen here so far, the mmWave link outperforms the UHF link up to the point that at such high bandwidht mmWave links does not require to incorporate pilot reuse into the network, since the network gives virtually similar results for all the values of K used, both for $Q = 1$ and $Q = 3$.

1.6 The pilot mitigation problem in the 5G 3GPP standard

The concepts seen so far are applied to the commercial standards of the latest wireless communication systems, starting from the 4G precursors, where CSI is acquired through pilots in a so-called Sounding Reference Signal (SRS) scheme, which is still considered the main candidate to carry UL massive MIMO pilots in TDD systems.

However, as we previously mentioned, SRS reuse is the main cause of pilot contamination and the approaches described above are some of the possible solutions for it. The most recently adopted solutions try to optimize

the pilot reuse schemes while keeping the training overhead under control, in a sort of pilot-based approach. In [8] Giordano *et al.* focus on these schemes, evaluating their performance and highlighting the best one. In particular, they focus on UL SRSs that span the entire bandwidth to allow a wideband channel sounding and consider a 2× time repetition factor as well as 8 possible cyclic shifts of the SRS, such that a maximum of 16 SRS can be multiplexed in one OFDM symbol. 5G standardisation is currently discussing whether amendments to this framework are needed to effectively support massive MIMO applications.

1.6.1 The SRS coordination - Fixed Reuse

The already well known pilot reuse schemes are named *Reuse 1* and *Reuse 3* and depending on them we can obtain two different upper bounds in the expression:

$$N_{T,b} \leq \left\lfloor \frac{N_{P,\tau}}{3\beta_{PR} + \beta_{SH}} \right\rfloor \tag{1.622}$$

which represents the number $N_{T,b}$ of scheduled UTs at the BS b, considering a maximum of $N_{P,\tau}$ orthogonal SRSs and τ OFDM symbols. Here, the parameter accounting for the reuse scheme type is $\beta_{PR} \in [0, 1]$ and denotes the fraction of protected SRS sequences, which in turn are orthogonal among UTs served by different BSs. With this, $\beta_{SH} = 1 - \beta_{PR}$ is the remaining fraction of sequences that can be reused across the sectors of the same deployment site.

In particular, in the *Reuse 1* ($\beta_{PR} = 0$) scheme all UTs scheduled by all BSs share the entire set of SRSs, but since orthogonality is only guaranteed among UTs associated with the same BS, pilots among UTs connected to different BSs are not orthogonal. The consequences of it are that a larger number of UTs is multiplexed, but there is a more severe pilot contamination.

With *Reuse 3* ($\beta_{PR} = 1$) three co-located BS sectors within the same cell site use three different and orthogonal sets of SRSs, such that pilot orthogonality is preserved across the entire cell site. Therefore this scheme leads to lower pilot contamination with respect to *Reuse 1* scheme, even though this effect comes at the expense of training only one third of the UEs given a fixed τ.

1.6.2 The SRS coordination - Fractional Reuse

The tradeoff between the previous schemes is represented by the so-called *Fractional Reuse (FR)*, in which *Reuse 3* is applied for a specific fraction of UTs β_{PR} and the *Reuse 1* for the remaining fraction

β_{SH}, with the result of being able to multiplex a larger number of sequences than *Reuse 3* while providing less pilot contamination than *Reuse 1*.

The two main FR reuse schemes are:

- The **Cell-centric Fractional Reuse (FR-CC)**

  It draws the attention of the UTs located at the cell's edges: each BS helps them since their SRSs reach it with low power and can potentially suffer from neighboring UTs contamination. The implementation of it can consist in ranking all UTs according to increasing values of power $p_{i,b}$ that BS b receives from UT i and then assigning the protected SRS resources to the top fraction β_{PR} of UTs, whereas the shared SRS resources are assigned to the bottom β_{SH} fraction of UTs;

- The **Neighbour-aware Fractional Reuse (FR-NA)**

  This strategy instead suggests to assign the protected SRSs to the UTs that generate the most interference to neighboring BSs and can be implemented by ranking all scheduled UTs according to increasing values of the maximum power $\max_{j \in \mathcal{B}} b\{p_{i,j}\}$ that UT i receives from all other BSs. This with the consequence that, in the same way as the previous point, the protected SRS resources are assigned to the top fraction η_{PR} of UTs, while the shared ones are assigned to the remaining β_{SH} fraction of UTs [8].

Bibliography

[1] T. L. Marzetta, "Noncooperative Cellular Wireless with Unlimited Numbers of Base Station Antennas," *IEEE Transactions on Wireless Communications*, vol. 9, no. 11, pp. 3590–3600, 2010.

[2] O. Elijah, S. Member, C. Y. Leow, T. A. Rahman, S. Nunoo, and S. Z. Iliya, "A Comprehensive Survey of Pilot Contamination in Massive MIMO — 5G System," *IEEE Communications Surveys & Tutorials*, vol. 18, no. 2, pp. 905–923, 2016.

[3] E. Björnson, J. Hoydis, and M. Kountouris, "Massive MIMO Systems With Non-Ideal Hardware : Energy Efficiency , Estimation , and Capacity Limits," *IEEE Transactions on Information Theory*, vol. 60, no. 11, pp. 7112–7139, 2014.

[4] S. Buzzi and C. D. Andrea, "Massive MIMO 5G Cellular Networks : mm-wave vs . μ-wave Frequencies," 2017.

[5] R. M. Ralf and L. Cottatellucci, "Blind Pilot Decontamination," vol. 9, no. 1.

[6] R. M. Ralf, "Channel Modelling of MU-MIMO Systems by Quaternionic Free Probability," no. 4, pp. 2656–2660, 2012.

[7] S. Ahsan, R. Naqvi, S. A. Hassan, and Z. Mulk, "Pilot Reuse & Sum Rate Analysis of mmWave & UHF-based Massive MIMO Systems," *2016 IEEE 83rd Vehicular Technology Conference (VTC Spring)*, pp. 1–5, 2016.

[8] L. G. Giordano, L. Campanalonga, L. David, A. Garcia-rodriguez, N. Bell, L. Ireland, N. Bell, and L. Germany, "Uplink Sounding Reference Signal Coordination to Combat Pilot Contamination in 5G Massive MIMO,"